Extraction of G_E^p from a double-polarization measurement of two-body ^{3}He breakup

W. Bertozzi, Z. Chai, O. Gayou, S. Gilad, B. Ma, P. Monaghan, Y. Qiang, L. Wan, Y. Xiao, C. Zhang
Laboratory for Nuclear Science, Massachusetts Institute of Technology, Cambridge, MA

Z.-L. Zhou
Schlumberger-Doll Research, Ridgefield, CT

S. Širca[1]
Dept. of Physics, University of Ljubljana, Slovenia

D. W. Higinbotham
Thomas Jefferson National Accelerator Facility, Newport News, VA

[1]Contact person; e-mail: simon.sirca@fmf.uni-lj.si

Abstract

We propose to determine the proton electric form-factor G_E^p at high Q^2 by measuring the transverse asymmetry A_x in the $^3\vec{\mathrm{He}}(\vec{\mathrm{e}},\mathrm{e}'\mathrm{p})\mathrm{d}$ reaction. We present a double-polarization approach distinct both from a cross-section measurement and recoil polarimetry. As the key instrument we propose to use the two-body breakup of polarized ^{3}He acting as an effective polarized *proton* target.

Contents

1 Introduction

The elastic form-factors probe the charge and magnetization distributions of the nucleon, and provide stringent tests on models of nucleon structure. Until recently, data on the proton elastic form-factors came predominantly from cross-section measurements, applying the Rosenbluth method to separate the electric (G_E^p) and magnetic (G_M^p) from the elastic scattering cross-section

$$\frac{d\sigma}{d\Omega} = \frac{\sigma_{Mott}}{1+\tau}\left[\left(G_E^p\right)^2 + \frac{\tau}{\varepsilon}\left(G_M^p\right)^2\right] . \tag{1}$$

Here σ_{Mott} is the Mott cross-section for scattering of electrons from a point-like proton, $\varepsilon = (1 + 2(1+\tau)\tan^2(\theta_e/2))^{-1}$ is polarization of the virtual photon, $\tau \equiv Q^2/4M_p^2$, while G_E^p and G_M^p are the Sachs form-factors of the proton. Because the electric term dominates the cross-section at low Q^2, and the magnetic term takes over at large Q^2, it becomes increasingly difficult to extract G_M^p at low Q^2 and G_E^p at high Q^2 [1]. A good global fit to the world data from unpolarized measurements is obtained by using the traditional dipole form $G_M^p(Q^2) \simeq 1/(1+Q^2/\Lambda^2)^2$ with $\Lambda^2 = 0.71\,(\mathrm{GeV/c})^2$, and with a constant ratio $\mu_p G_E^p(Q^2)/G_M^p(Q^2) \simeq 1$ for all Q^2.

More recently, recoil-polarimetry techniques [2, 3] have been utilized to extract the G_E^p/G_M^p ratio by measuring the polarization components of the recoiling protons in the $p(\vec{e}, e'\vec{p})$ process. The form-factor ratio is given by the ratio of the transverse and longitudinal polarization components times the kinematic factors:

$$\frac{G_E^p}{G_M^p} = -\frac{P_t}{P_l}\frac{E_e + E_e'}{2M_p}\tan\frac{\theta_e}{2} , \tag{2}$$

and suffers from very different systematical uncertainties than the Rosenbluth technique. The data show a linear fall-off which can be parameterized as

$$\mu_p G_E^p/G_M^p = 1 - 0.13\,(Q^2 - 0.04\,(\mathrm{GeV/c})^2) .$$

Figure 1 shows the results of these two approaches. It is clear that the data sets are in significant disagreement above $Q^2 \sim 1\,(\mathrm{GeV/c})^2$), which is the region where both techniques still yield relatively high-precision results. Even with the latest "super-Rosenbluth" data [4], the discrepancy seems to persist.

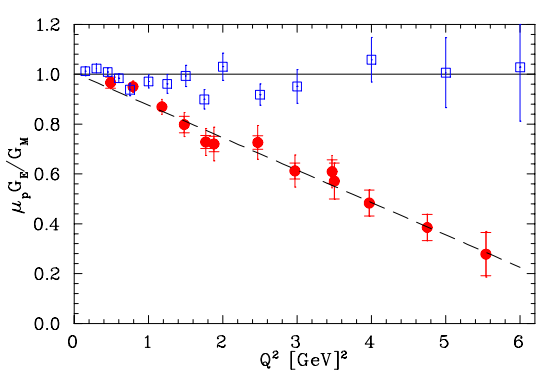

Fig. 1 — The $\mu_p G_E^p/G_M^p$ ratio from cross-section measurements (empty symbols) and polarization experiments (full symbols).

2 Physics motivation

The discrepancy between the Rosenbluth and extractions of G_E^p/G_M^p involving polarization degrees of freedom indicates that at least one group of experiments, or one of the experimental techniques, may involve a significant unaccounted for systematical error, or previously unknown contributions to the cross-section.

The urgent need for a resolution of the apparent discrepancy has recently initiated a heated discussion. One of the approaches [5] suggests that the disagreement can be explained by the increasing importance of the two-photon exchange contribution at high Q^2, becoming relatively kinematically enhanced in the Rosenbluth method while remaining small for the polarization method. However, other authors starting from the same postulate [6] have found that the inclusion of the two-photon contribution only partly reconciles the two techniques. However, one should note that numerous tests of the validity of the one-photon approximation have been done in the past, mostly by checking the linearity of the Rosenbluth formula, and by checking the charge invariance of the electro-magnetic interaction by comparing e^-p to e^+p scattering. Starting from first principles such as the C-invariance and the crossing symmetry, it has been shown in [7] that the presence of the two-photon mechanism destroys the linearity of the Rosenbluth separation but does not affect the terms related to the electro-magnetic form factors. Trying to best combine data from the Rosenbluth and polarization techniques, and taking into account various assumptions, several global fits to the available G_E^p/G_M^p data set have been performed [8]. We use some of these fits below.

The prime motivation of our proposal is to present a third approach which does not rely on recoil polarimetry. As the key instrument we shall use the two-body breakup of polarized ^{3}He acting as an effective polarized proton target to measure double-polarization asymmetries A_x and A_z. The former will give access to G_E^p while the latter will utilize the relatively good knowledge of G_M^p and serve as a polarimeter.

2.1 $^3\vec{\mathrm{He}}$ as an effective polarized proton target

The ^{3}He nucleus is a calculable nuclear system where our theoretical understanding of its structure can be compared with data to an increasingly accurate degree [9]. It is generally thought that polarized ^{3}He can serve as an effective polarized neutron target [10, 11, 12]. Namely, non-relativistic Faddeev calculations [11, 13, 14] of the three-body bound state predict that three components dominate the ^{3}He ground-state wave-function. The dominant component of the ^{3}He wave function is the spatially symmetric S state, in which the proton spins are in the spin-singlet state (anti-parallel) and the ^{3}He spin is predominantly carried by the neutron. This configuration accounts for $\simeq 90\,\%$ of the spin-averaged wave-function. The additional $\simeq 8\,\%$ of the spin-averaged wave-function can be attributed to the D state generated by the tensor component of the nucleon-nucleon force, while the remaining $\simeq 2\,\%$ originate in a mixed-symmetry configuration of the nucleons, the S' state arising because of the differences between the $T = 0$ and $T = 1$ forces [14, 15]. In this physical picture, polarized ^{3}He represents an effective polarized neutron target. Numerous experiments based on this idealization have been performed with the goal of studying the spin structure of the neutron and its form-factors. Moreover, there is an approved Hall A experiment [28] devoted entirely to the exploration of the ^{3}He system by studying the S'-state and D-state contributions to the ^{3}He ground-state wave-function.

On the other hand, angular momenta of the deuteron and proton in a two-body breakup process $^3\vec{\mathrm{He}}(\vec{\mathrm{e}},\mathrm{e}'\mathrm{p})\mathrm{d}$ couple to the total ^{3}He spin of $(\frac{1}{2},\frac{1}{2})$ like

$$\left|\tfrac{1}{2},\tfrac{1}{2}\right\rangle = \sqrt{\frac{2}{3}}\,\left|1,1\right\rangle \otimes \left|\tfrac{1}{2},-\tfrac{1}{2}\right\rangle - \sqrt{\frac{1}{3}}\,\left|1,0\right\rangle \otimes \left|\tfrac{1}{2},\tfrac{1}{2}\right\rangle\,,$$

corresponding to an effective relative polarization of the proton of $-\frac{1}{3}$. The situation is illustrated in Fig. 2. The double-polarization *quasi-elastic* asymmetries measured at small missing momenta of the outgoing proton ($p_{\mathrm{miss}} \lesssim 100\,\mathrm{MeV/c}$) then almost directly correspond to e-p *elastic* asymmetries with a reduced proton polarization. With a typical value of $P(^3\mathrm{He}) \sim 35\,\%$, we end up with a net proton polarization of

$$P_{\mathrm{p}} = P(^3\mathrm{He}) \cdot (-\tfrac{1}{3}) \sim -12\,\%\,.$$

Measuring the transverse and longitudinal asymmetries A_x and A_z in the two-body breakup process and their ratios therefore provide an independent means to access the $G_{\mathrm{E}}^{\mathrm{p}}/G_{\mathrm{M}}^{\mathrm{p}}$ ratio (see formalism below), with a systematics completely different from the recoil-polarization measurements. However, by taking the ratios, the influence of uncertainties in the proton polarization will be diminished by the same token as in the recoil-polarimetry experiments.

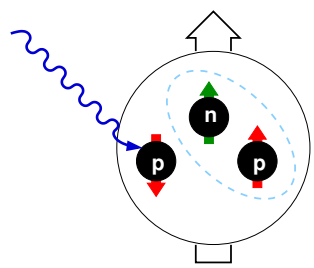

Fig. 2 — The two-body breakup of the dominant (S-state) configuration of the ^{3}He ground-state wavefunction renders polarized ^{3}He an effective polarized proton target with $\sim -1/3$ polarization.

The proposed experiment requires two major conditions to be met: one needs high-resolution spectrometers so that two-body breakup events can be cleanly separated from the three-body breakup; and one needs high luminosities so that the counting rates are feasible in the $2.0 \lesssim Q^2 \lesssim 3.5\,(\mathrm{GeV/c})^2$ range since the effective target polarization $\sim 12\,\%$. Focusing on regions of small p_{miss}, these demands make Hall A and its high-pressure polarized ^{3}He target the best choice.

2.2 Relation to other JLab experiments

There is a related proposal being submitted to this PAC by the Hall C Collaboration to measure the $G_{\mathrm{E}}^{\mathrm{p}}/G_{\mathrm{M}}^{\mathrm{p}}$ ratio via double-polarized, single-arm $\vec{\mathrm{p}}(\vec{\mathrm{e}},\mathrm{e}')$ scattering at Q^2 of 2.1 and $3.5\,(\mathrm{GeV/c})^2$, by using the polarized NH_3 target. Their experiment proposes to access the form-factor ratio from a particular combination of transverse and longitudinal asymmetries (i.e. involving polar spin angles differing from 0° and 90°) which minimizes the extraction uncertainty. It presents a methodical improvement over an older (deferred) proposal PR–01–105 [29], although it is based essentially on the same technique.

Our proposed technique possesses a comparable figure-of-merit (roughly 1/10 of the target polarization with respect to the NH_3 target and roughly 100-times the usable beam current),

and at the same time an excellent control over instrumental systematics. We believe that the two independent double-polarization techniques utilized in the two Halls are commensurate and would provide a better control over the ambiguities of the form-factor Q^2-dependence.

3 Formalism of $\vec{e}$-$\vec{p}$ elastic scattering

The elastic form-factors of the proton can be determined by measuring the asymmetries in the scattering of longitudinally polarized electrons off a polarized proton target. The schematic view of spin-dependent elastic scattering is shown in Fig. 3.

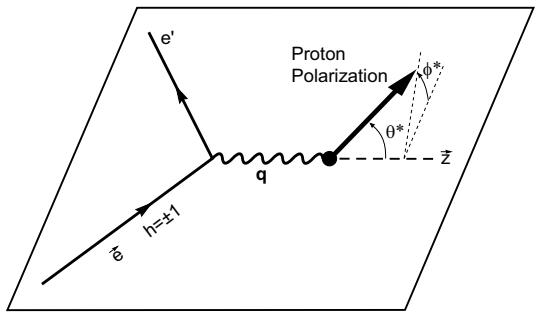

Fig. 3 — Schematic representation of the spin-dependent electron-proton elastic scattering.

The differential cross-section can be written in the form [16]

$$\frac{d\sigma}{d\Omega} = \Sigma + h\Delta \,.$$

The Σ is the spin-independent part given by Eq. 1 The spin-dependent part Δ depends on the electron helicity h and has the form

$$\Delta \equiv -\sigma_{\mathrm{Mott}} \left[2\tau v_{\mathrm{T}'} \cos\theta^\star \left(G_{\mathrm{M}}^{\mathrm{p}}\right)^2 - 2\sqrt{2\tau(1+\tau)}\, v_{\mathrm{TL}'} \sin\theta^\star \cos\phi^\star G_{\mathrm{E}}^{\mathrm{p}} G_{\mathrm{M}}^{\mathrm{p}} \right] ,$$

where $\theta^\star$ and $\phi^\star$ are the polar and azimuthal proton spin orientation angles defined with respect to the three-momentum transfer $\boldsymbol{q}$ and the scattering plane, while $v_{\mathrm{T}'}$ and $v_{\mathrm{TL}'}$ are kinematic factors [16].

The spin-dependent asymmetry A is defined as

$$A \equiv \frac{\sigma(h+) - \sigma(h-)}{\sigma(h+) + \sigma(h-)} \,, \tag{3}$$

where $\sigma(h\pm)$ denotes the differential cross-sections for the $\pm$ helicities of the polarized electron beam. The asymmetry A can be written in the form

$$A \equiv \frac{\Delta}{\Sigma} = -\frac{2\tau v_{\mathrm{T}'} \cos\theta^\star \left(G_{\mathrm{M}}^{\mathrm{p}}\right)^2 - 2\sqrt{2\tau(1+\tau)}\, v_{\mathrm{TL}'} \sin\theta^\star \cos\phi^\star G_{\mathrm{E}}^{\mathrm{p}} G_{\mathrm{M}}^{\mathrm{p}}}{(1+\tau) v_{\mathrm{L}} \left(G_{\mathrm{E}}^{\mathrm{p}}\right)^2 + 2\tau v_{\mathrm{T}} \left(G_{\mathrm{M}}^{\mathrm{p}}\right)^2} \,. \tag{4}$$

The measured asymmetry A_{exp} is related to the physical asymmetry A through $A_{\mathrm{exp}} = P_{\mathrm{e}} P_{\mathrm{t}} A$, where P_{e} and P_{t} are the degrees of polarization of the beam and target, respectively. We define

$$\begin{aligned} A_x &\equiv A(\theta^\star = 90^\circ, \phi^\star = 0^\circ) \,, \\ A_z &\equiv A(\theta^\star = 0^\circ) \,. \end{aligned}$$

4 Choice of kinematics

The choice of the beam energy is driven by a statistics trade-off: increasing E_{beam} yields larger rates, yet diminishes the size of the asymmetries (see Fig. 4). In addition, E_{beam} in principle needs to be kept low enough to maintain a sufficient missing-mass resolution and hence guarantee a good separation of two- and three-body breakup. On the other hand, this has a detrimental effect on the counting rates.

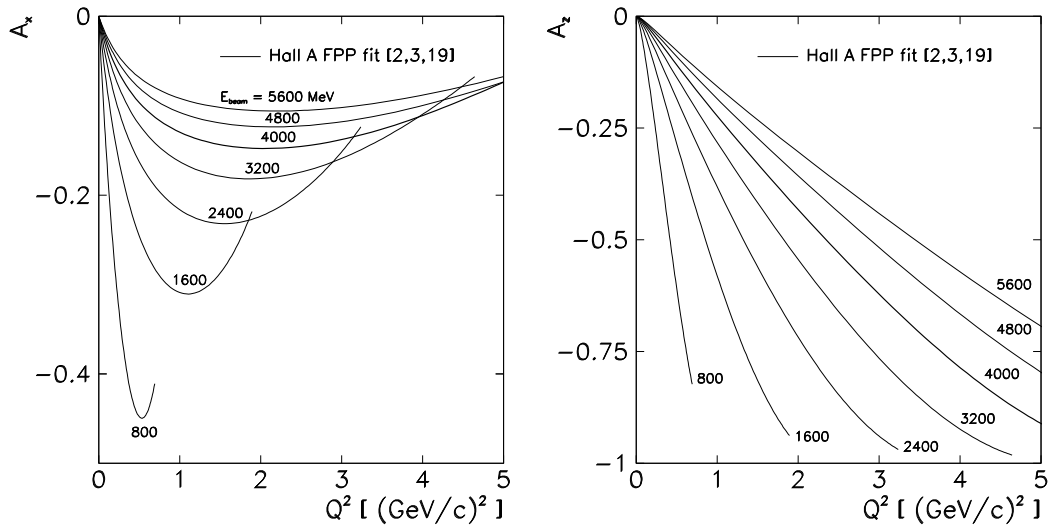

Fig. 4 — Asymmetries A_x and A_z as functions of Q^2 for different beam energies, with the parameterization of elastic form-factors based on the FPP results of Hall A. For a fixed Q^2, asymmetries decrease with increasing beam energy because the corresponding elastic scattering angles decrease.

For reasons listed below, we propose to measure the production kinematics at high Q^2 with the highest presently available beam energy of $E_{\text{beam}} = 5600\,\text{MeV}$, while the calibration measurements will be performed at $E_{\text{beam}} = 2400\,\text{MeV}$. The kinematics are listed in Table 1.

Table 1 — Proposed central kinematics for production running at high Q^2 at the beam energy of 5600 MeV. The additional setting at low Q^2 and a part of the setting at high Q^2 are needed to control systematics by polarimetry (determining the product of target and beam polarizations).

E_{beam} [MeV]	Q^2 [(GeV/c)^2]	E'_{e} [MeV]	θ_{e} [°]	p_{p} [MeV/c]	θ_{p} [°] [MeV/c]
2400	0.3	2240.0	13.6	570	67.1
5600	3.0	4001.2	21.1	2356	37.6

Since the results of our proposed experiment can be to some extent considered complementary to the proposed Hall C experiment, we strive to a joint lever-arm in Q^2 adequate to maximize the information on the Q^2-dependence of the asymmetries. One of the reasons for the choice of the high Q^2 is therefore to lie roughly symmetrically between the 2.1 and 3.5 (GeV/c)^2 data points of the Hall C proposal. The exact mid-point of 2.8 (GeV/c)^2 or a further increase in E_{beam} to match the one from Hall C could not be achieved due to the maximum momentum limitation of the HRS to $\sim 4\,\text{GeV/c}$. Note also that with a limitation to reasonable beam-times in the vicinity of $\sim 400\,\text{h}$ for A_x at high Q^2, a further increase of Q^2 is not feasible as the increasing

spread of the asymmetries due to different form-factor parameterizations is matched by the decrease in counting rate and the corresponding increase of statistical uncertainties.

A clean isolation of the two-body breakup is crucial for a good interpretability of our experiment. Figure 5 shows the missing-energy distribution of the state-of-the-art unpolarized ^{3}He(e, e′p) data taken in Hall A at $E_{\rm beam} = 4800\,$MeV and $p_{\rm miss} = 0$ [30]. Note that in the sense of the $E_{\rm miss}$ resolution, this Figure shows their *worst* kinematics. However, due to the high resolution of the HRS spectrometers, the two- and three-body contributions can be clearly separated even in such an unfavorable kinematical situation (large $E_{\rm beam}$ and $E'_{\rm e}$ which worsen the $E_{\rm miss}$ resolution), and are well under control in the Monte Carlo. In general, the three-body contribution remains small and is spread out in the $E_{\rm miss}$ spectrum beyond $E_{\rm miss} \simeq 7\,$MeV.

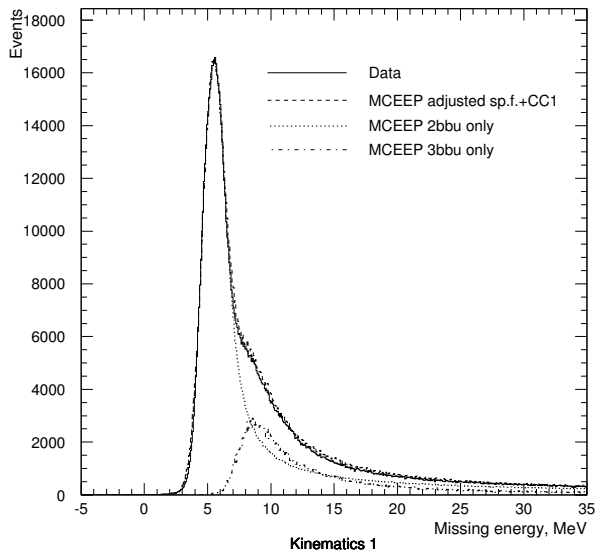

Fig. 5 — Missing-energy distribution of the ^{3}He(e, e′p) data taken at $E_{\rm beam} = 4800\,$MeV and $p_{\rm miss} = 0$ [30]. The kinematics were $E'_{\rm e} = 3966\,$MeV, $\theta_{\rm e} = 16.4^\circ$ (corresponding to $Q^2 = 1.55\,({\rm GeV/c})^2$), $p_{\rm p} = 1500\,$MeV/c, and $\theta_{\rm p} = 48.3^\circ$. In terms of contributions of $E'_{\rm e}$ and $p_{\rm p}$ to the $E_{\rm miss}$ resolution, these kinematics are comparable to our high-Q^2 setting.

The protons will be detected in parallel kinematics. In the Monte-Carlo simulation, this has been enforced by limiting the parallel and perpendicular acceptance in $|\boldsymbol{p}_{\rm miss}|$ below $100\,$MeV/c, while the two-body breakup has been selected by a $E_{\rm miss} < 7\,$MeV cut. We anticipate that more accurate calculations by J.-M. Laget on the quality of the former approximation will be performed in the near future.

Apart from the small dilution of the asymmetries through its $E_{\rm miss}$-strength, the three-body contribution entails an important problem of the modification of the proton polarization. Unfortunately, the three-body contribution to the polarization is to some extent model-dependent (choice of NN-potential), and also varies rapidly with $p_{\rm miss}$. However, there are indications [31, 32] that this contribution is either consistent with zero (causing only rate and asymmetry dilutions) or small but positive (causing distortions of the two-body asymmetries). We propose to subtract the theoretical three-body contribution from the measured total asymmetries. We believe that a correction with a few-percent model uncertainty on top of a few-percent three-body contamination will be negligible. With the use of modern NN-potentials (e.g. Paris) this approach should be sufficiently accurate and precise at $|\boldsymbol{p}_{\rm miss}| \lesssim 100\,$MeV/c.

In the following, we discuss the transverse and longitudinal asymmetries as functions of Q^2, for different parameterizations of proton elastic form-factors. Five parameterizations of the form-factors are shown in the figures: the traditional dipole form; the Mergell-Meißner-Drechsel fit [17]; two global fits based on the existing Rosenbluth and polarization data [2, 3, 18], and the fit based solely on the recent Hall A polarization data [2, 3, 19]. These fits are equivalent at small Q^2 but deviate significantly when Q^2 increases.

Figure 6 shows the transverse (left panel) and the longitudinal (right panel) asymmetry as a function of Q^2. The A_z is almost insensitive to the parameterization chosen and hence serves as a good "polarimeter". Since the G_M^p (related to A_z) is well-known relative to G_E^p, we will take only limited statistics for A_z at each Q^2. The longitudinal asymmetries will provide an additional control of systematics by determining the product of target and beam polarizations.

On the other hand, the dominant part of the statistics will be spent on the high-Q^2 value of A_x, with an additional small amount of beam-time at low Q^2. The A_x asymmetry exhibits a strong sensitivity to differentiate between different form-factor parameterizations, and is the key observable in our experiment. In the figures below, we also show the two proposed Hall C high-Q^2 data points. Since these data are to be taken at a slightly higher beam energy (6000 MeV), the asymmetries are slightly diminished. However, in the form-factor ratio of the Hall C proposal and the asymmetry ratio of our proposal (see Fig. 7 below), the Q^2-dependencies represent equivalent observables. Note that in the figures below, the asymmetries at low Q^2 are measured at a lower beam energy (see Table 1). Since the form-factors only depend on Q^2 (and not on E_{beam}), the asymmetries have been rescaled to the higher beam energy to be shown on the same plot.

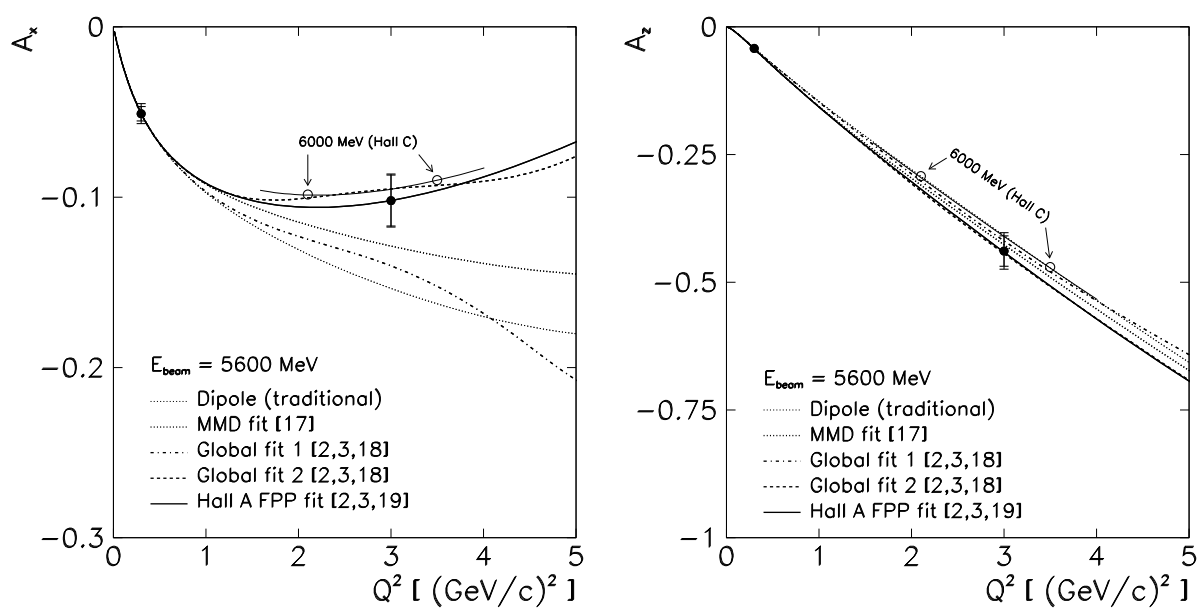

Fig. 6 — Transverse asymmetry $A_x(\theta^\star = 90°, \phi^\star = 0°)$ (left panel) and the longitudinal asymmetry $A_z(\theta^\star = 0°)$ as a function of Q^2, for different parameterizations of proton elastic form-factors (see text for details). Statistical and total uncertainties are shown for A_x and A_z. Only the systematical errors due to uncertainties in target and beam polarizations are included for A_z.

At low p_{miss}, the quasi-elastic process on the proton in the $^3\vec{\text{He}}(\vec{\text{e}}, \text{e}'\text{p})\text{d}$ reaction can be almost completely understood in terms of the elastic e-p scattering. Hence, the ratio of the

asymmetries A_x/A_z can be combined in a form resembling Eq. 2,

$$\frac{G_{\rm E}^{\rm p}}{G_{\rm M}^{\rm p}} = \frac{1}{\mu_{\rm p}}\frac{A_x}{A_z} f_{\rm AG} \equiv \frac{A_x}{A_z}\sqrt{\tau + \tau(1+\tau)\,\tan^2(\theta_{\rm e}/2)}\,. \tag{5}$$

The corresponding ratio in our experiment is shown in Fig. 7. The obvious advantage of this approach is that the knowledge of the exact proton polarization within $^3\vec{\rm He}$ is not needed as it cancels in the ratio (5). With a good theoretical knowledge of A_z via $G_{\rm M}^{\rm p}$, and controlled by using polarimetry, A_x will be used to determine the unknown $G_{\rm E}^{\rm p}$.

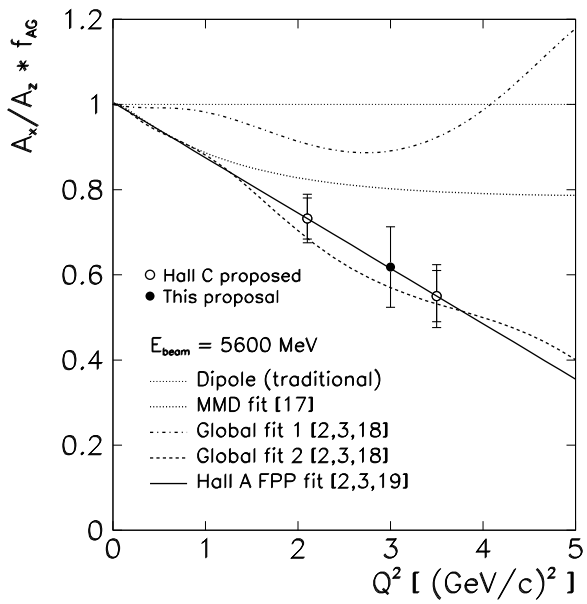

Fig. 7 — The scaled ratio $\mu_{\rm p}(A_x/A_z)(\tau + \tau(1+\tau)\,\tan^2(\theta_{\rm e}/2))^{1/2}$ corresponding to $\mu_{\rm p}G_{\rm E}^{\rm p}/G_{\rm M}^{\rm p}$ as a function of Q^2, for different parameterizations of proton elastic form-factors. Since our experiment is statistics-dominated, the proposed point at $Q^2 = 3.0\,({\rm GeV/c})^2$ is shown with statistical error only. The two proposed Hall C data points are shown with statistical and total errors.

5 Experimental equipment and methods

We plan to use a beam energy of 5.6 GeV. We will use the standard high-pressure polarized ^{3}He target in Hall A and polarized beam. The scattered electrons will be detected in one of the HRS in coincidence with the knocked-out protons detected in the other HRS.

5.1 Choice of the polarized target

While an isotopically pure high-density polarized hydrogen target does not exist, only a handful of conventional alternatives are available: low-intensity gaseous targets based on atomic beam sources (e.g. in BLAST at MIT-Bates); ammonia (NH_3) targets; and frozen-spin (HD) targets. Each has drawbacks and advantages of its own. Yet the ability to freely rotate the target spin angle, the demand for a precise knowledge of the target polarization, and the large-luminosity requirement of our experiment dictates the use of the polarized ^{3}He target.

The NH_3 target is based on the mechanism of dynamical nuclear polarization. The target material is doped, with paramagnetic centers (unpaired electrons) which are nearly 100 % polarized at temperatures around 1 K and magnetic field densities around 5 T. By irradiation of the target material with microwaves (typically at 140 GHz), most of the electron polarization is transferred to the protons in the material. Protons can be polarized of almost 100 % in this target. However, the large magnetic fields may mis-steer the beam and affect the optics of outgoing particles. In addition, the asymmetries obtainable from NH_3 are diluted by unpolarized target materials, and the maximum attainable luminosity on the order of $10^{35}/\mathrm{cm}^2\mathrm{s}$ are limited by the maximum beam current of $\sim$ 100 nA. Most importantly, the polarization axis can be oriented in a less flexible way and reversed less infrequently, thereby possibly increasing the systematical uncertainty.

We believe that the best choice of the polarized target is the polarized ^{3}He acting as an effective p-d system similar in nature to the HD frozen-spin target. The main advantage of former is that it is a pure, high-pressure (10 bar) gaseous target which can sustain high beam currents (up to 15 μA), resulting in a high maximum luminosity of $8 \cdot 10^{35}/\mathrm{cm}^2\mathrm{s}$. The effective net proton polarization is $\sim$ 12 %, which is sufficiently high for the proposed experiment.

5.2 Polarized ^{3}He target

For the reasons enumerated above, we will use the high-pressure polarized ^{3}He target which uses optically pumped Rubidium vapor to polarize the ^{3}He nuclei through spin-exchange collisions [20, 21]. It has been successfully used in a series of experiments in Hall A, E–94–010 [22], E–95–001 [23], E–97–103 [24], E–99–117 [25], and, most recently, in E–97–110 [26].

Optical pumping will be achieved with multiple diode lasers with a power of 30 W each, at a tunable wave-length around 795 nm. The target density will be about $2.7 \cdot 10^{20}/\mathrm{cm}^3$ corresponding to a pressure of about 10 bar during normal operation. The target window thicknesses are known from mechanical and optical measurements with uncertainties better than 1.0 %, which is important for a proper understanding of radiative energy losses. The background from the nitrogen admixture will be measured by using an equivalent dummy target, and subtracted. In previous experiments, this contribution was found to be relatively small (on the order of a few percent).

The proposed experiment requires a flexible alignment of the target polarization vector parallel to (for the A_z asymmetry) or perpendicular to (for the A_x asymmetry) the direction of momentum transfer. Two pairs of Helmholtz coils provide the necessary quantization axis by supplying a variable static holding field of about $2-4$ mT which can be rotated in the horizontal plane. The careful alignment of the coils assures that the polarization relaxation caused by the $\sim 1/B^2$ field inhomogeneities is minimized.

The target polarization P_t will be monitored with a nuclear magnetic resonance (NMR) system using the method of adiabatic fast passage (AFP). For the past experiments, the response of the NMR system for ^{3}He has been calibrated with the NMR measurements on water. The calibration was independently verified by measurements of the frequency shifts in the lines of electron paramagnetic resonance (EPR) spectra caused by polarized ^{3}He nuclei [27]. The calibration constants from these independent determinations are well known, and are consistent to within 2 %. The expected total uncertainty from the direct polarization measurements is expected to be smaller than 4 % and will be dominated by the uncertainties in the target density.

Based on the experience of previous experiments, target polarizations of 35 – 40 % can be achieved for beam currents not exceeding 10 – 15 μA. We assume a realistic target polarization of 40 % and a beam current of 12 μA at 75 % polarization. The designed maximum luminosity of $8 \cdot 10^{35}/\mathrm{cm}^2\mathrm{s}$ is computed for the 40-cm target cell. However, only a fraction of the extended target acceptance in z_{tg} is visible to the HRS. In our rate calculations, a shorter target cell length of 25 cm has been used, and the positioning of the HRS at non-90° angles has been accounted for using MCEEP.

5.3 High-Resolution Spectrometers

One of the HRS will be used to detect the electrons scattered from the $^3\vec{\mathrm{He}}(\vec{\mathrm{e}},\mathrm{e}'\mathrm{p})\mathrm{d}$ reaction. The angular resolution is $\simeq$ 0.6 mr in the non-dispersive plane and $\simeq$ 2.0 mr in the dispersive plane. The momentum acceptance is ±4.5 %, and the angular acceptance is ±60 mr in the dispersive plane and ±22 mr in the non-dispersive plane. The other HRS will be used to detect the ejected protons.

6 Counting rates and beam-time request

Figure 8 shows the elastic cross-sections for different beam energies and for different parameterizations of proton elastic form-factors. As all parameterizations give almost identical cross-sections in the Q^2-range of this proposal, the choice of the particular form is of little importance in rate estimates. The Hall A FPP fit has been used in the Monte Carlo.

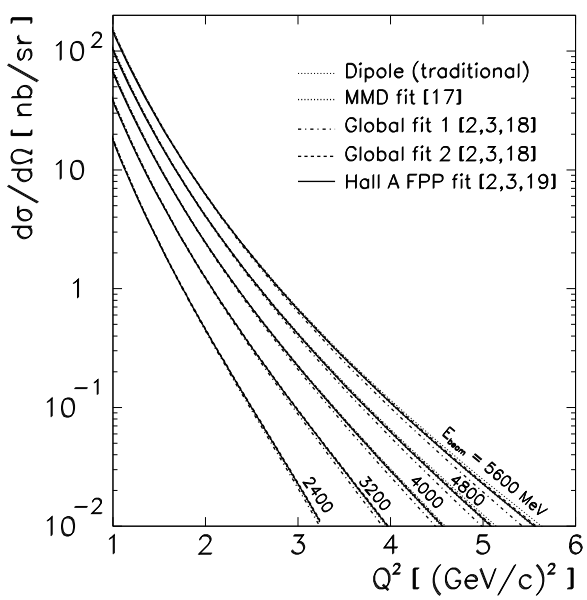

Fig. 8 — Elastic e-p cross-section as a function of Q^2 for different beam energies E_{beam} = 2400, 3200, 4000, 4800, and 5600 MeV, for different parameterizations of proton elastic form-factors (see text for details).

Table 2 — Estimated coincident rates for the proposed production kinematics at $E_{\mathrm{beam}} = 5600\,\mathrm{MeV}$ and auxiliary (polarimetry) kinematics at $E_{\mathrm{beam}} = 2400\,\mathrm{MeV}$.

E_{beam} [MeV]	Q^2 [(GeV/c)^2]	θ_{e} [°]	θ_{p} [°]	(ep) [Hz]
2400	0.3	13.6	67.1	32.2
5600	3.0	21.1	37.6	0.312

Table 3 — The coincidence rates, absolute statistical uncertainties on the asymmetries A_x, absolute systematics uncertainties on A_z (only due to beam and target polarization), the relative uncertainty of the form-factor ratio, and the beam-time request.

Q^2	(e, e′p) [Hz]	$A_x \pm \Delta A_x$	$A_z \pm \Delta A_z$	$\Delta(G_{\mathrm{E}}^{\mathrm{p}}/G_{\mathrm{M}}^{\mathrm{p}})$	Time [h]
0.3	32.2	-0.051 ± 0.001	-0.042 ± 0.003	n/a	25 + 25
3.0	0.312	-0.102 ± 0.015	-0.439 ± 0.030	15 %	400 + 100
	NMR, EPR				8
	Møller				8
	E_{e}				4
Total					570

6.1 Systematical uncertainties

The statistical uncertainties dominate in the proposed experiment. The systematic errors are mainly caused by the uncertainties in the polarization of the beam ($\lesssim$ 2 %) and the target ($\lesssim$ 4 %). The experimental polarimetry measured through A_z will be cross-checked with the theoretical parameterization of $G_{\mathrm{M}}^{\mathrm{p}}$. The systematical errors originating in theoretical uncertainties due to the three-body distortion of the asymmetries were assumed to be negligible for the purposes of this Letter.

7 Conclusions

We believe that the nucleon electric form-factor $G_{\mathrm{E}}^{\mathrm{p}}$ at high Q^2 can be determined by measuring the transverse double-polarization asymmetry A_x in the $^3\vec{\mathrm{He}}(\vec{\mathrm{e}}, \mathrm{e}'\mathrm{p})\mathrm{d}$ reaction, combined with the theoretical knowledge of the longitudinal asymmetry A_z which is well-known via $G_{\mathrm{M}}^{\mathrm{p}}$. This approach does not suffer from the systematical uncertainties attributed to cross-section measurements, and does not depend on recoil polarimetry. Combined with the possible forthcoming data from the NH_3 experiment in Hall C we see this experiment as a complementary yet independent tool to investigate the persistent discrepancies among different extractions of the form-factor Q^2-dependence.

References

[1] H. Gao, Int. J. Mod. Phys. E **12** (2003) 1.

[2] M. Jones et al., Phys. Rev. Lett. **84** (2001) 1398.

[3] O. Gayou et al., Phys. Rev. Lett. **88** (2002) 092301.

[4] J. Arrington, R. Segel (spokespersons), JLab Experiment E–01–001, "*New measurement of the G_E/G_M for the proton*", 2001.

[5] P.A.M. Guichon, M. Vanderhaeghen, e-Print Archive: hep-ph/0306007.

[6] P.G. Blunden, W. Melnitchouk, J.A. Tjon, e-Print Archive: nucl-th/0306076.

[7] M.P. Rekalo, E. Tomasi-Gustafsson, e-Print Archive: nucl-th/0307066.

[8] J. Arrington, e-Print Archive: nucl-ex/0205019.

[9] J. Carlson, R. Schiavilla, Rev. Mod. Phys. **70** (1998) 743.

[10] H. Gao, Nucl. Phys. A **631** (1998) 170c.

[11] J. L. Friar et al., Phys. Rev. C **42** (1990) 2310.

[12] R. G. Milner, in *Proceedings of the Workshop on Polarized* ^{3}He *Beams and Targets*, R. W. Dunford, F. P. Calaprice (eds.), AIP 131, New York, 1984, p. 186.

[13] B. Blankleider and R. M. Woloshyn, Phys. Rev. C **29** (1984) 539.

[14] R. W. Schulze and P. U. Sauer, Phys. Rev. C **48** (1993) 38.

[15] J. Friar, in *Electronuclear Physics with Internal Targets and the BLAST Detector*, R. Alarcon and M. Butler (eds.), World Scientific, Singapore, 1993, p. 210.

[16] T. W. Donnelly, A. S. Raskin, Ann. Phys. **169** (1986) 247.

[17] P. Mergell, U.-G. Meißner, D. Drechsel, Nucl. Phys. A **596** (1996) 367.

[18] J. Arrington, e-Print Archive: nucl-ex/0309011; J. Arrington, Phys. Rev. C **68** (2003) 034325; J. Arrington, Eur. Phys. J. A **17** (2003) 311.

[19] E. J. Brash, A. Kozlov, Sh. Li, G. M. Huber, Phys. Rev. C **65** (2002) 051001(R).

[20] T. G. Walker, W. Happer, Rev. Mod. Phys. **69** (1997) 629.

[21] S. Appelt et al., Phys. Rev. A **58** (1998) 1412.

[22] Z. E. Meziani, G. Cates, J.-P. Chen (spokespersons), JLab Experiment E–94–010, "*Measurement of the neutron (^{3}He) spin structure function at low Q^2; a connection between the Bjorken and Drell-Hearn-Gerasimov sum rules*", 1994.

[23] H. Gao, J. O. Hansen (spokespersons), JLab Experiment E–95–001, "*Precise measurements of the inclusive spin-dependent quasi-elastic transverse asymmetry A'_T from ^{3}He(e, e') at low Q^2*", 1995.

[24] T. Averett, W. Korsch (spokespersons), JLab Experiment E–97–103, "*Search for higher-twist effects in the neutron spin structure function* $g_2^{\mathrm{n}}(x, Q^2)$", 1997.

[25] Z. E. Meziani, J.-P. Chen, P. Souder, JLab Experiment E–99–117, "*Precision measurement of the neutron asymmetry* A_1^{n} *at large* x *using CEBAF at* 6 GeV", 1999.

[26] J.-P. Chen, A. Deur, F. Garibaldi (spokespersons), JLab Experiment E–97–110, "*The GDH rule and the spin structure of* ^{3}He *and the neutron using nearly real photons*, 1997.

[27] M. V. Romalis, G. D. Cates, Phys. Rev. A **58** (1998) 3004.

[28] W. Bertozzi, D. Higinbotham, B. Norum, S. Širca, Z.-L. Zhou (spokespersons), *Measurement of* A_x *and* A_z *asymmetries in the quasi-elastic* $^3\vec{\mathrm{He}}(\vec{\mathrm{e}}, \mathrm{e}'\mathrm{d})$ *reaction*, JLab Experiment E–02–108, 2002.

[29] G. Warren, (spokesperson), JLab Proposal PR–01–105, "$G_{\mathrm{E}}^{\mathrm{p}}/G_{\mathrm{M}}^{\mathrm{p}}$ *via simultaneous asymmetry measurements of reaction* $\vec{\mathrm{p}}(\vec{\mathrm{e}}, \mathrm{e}')$, 2001.

[30] M. Rvachev, PhD Thesis, MIT, 2003.

[31] J.-M. Laget, Phys. Lett. B **276** (1992) 398; and Private Communication.

[32] S. Nagorny, W. Turchinetz, Phys. Lett. B **429** (1998) 222; and Private Communication.